http://tandfonline.com/inan
ISSN: 1743-5390 (print), 1743-5404 (electronic)

Nanotoxicology

Nanotoxicology, 2016; 10(4): 426–435
 DOI: 10.3109/17435390.2015.1073399

Taylor & Francis
Taylor & Francis Group

ORIGINAL ARTICLE

Anti-amyloid compounds protect from silica nanoparticle-induced neurotoxicity in the nematode *C. elegans*

Andrea Scharf[1], Karl-Heinz Gührs[2], and Anna von Mikecz[1]

[1]*IUF – Leibniz Research Institute for Environmental Medicine at the Heinrich-Heine-University Duesseldorf, Düsseldorf, Germany and* [2]*CF Proteomics, FLI-Leibniz-Institute for Age Research, Fritz-Lipman-Institute e.V., Jena, Germany*

Abstract

Identifying nanomaterial-bio-interactions are imperative due to the broad introduction of nanoparticle (NP) applications and their distribution. Here, we demonstrate that silica NPs effect widespread protein aggregation in the soil nematode *Caenorhabditis elegans* ranging from induction of amyloid in nucleoli of intestinal cells to facilitation of protein aggregation in body wall muscles and axons of neural cells. Proteomic screening revealed that exposure of adult *C. elegans* with silica NPs promotes segregation of proteins belonging to the gene ontology (GO) group of "protein folding, proteolysis and stress response" to an SDS-resistant aggregome network. Candidate proteins in this group include chaperones, heat shock proteins and subunits of the 26S proteasome which are all decisively involved in protein homeostasis. The pathway of protein homeostasis was validated as a major target of silica NPs by behavioral phenotyping, as inhibitors of amyloid formation rescued NP-induced defects of locomotory patterns and egg laying. The analysis of a reporter worm for serotonergic neural cells revealed that silica NP-induced protein aggregation likewise occurs in axons of HSN neurons, where presynaptic accumulation of serotonin, e.g. disturbed axonal transport reduces the capacity for neurotransmission and egg laying. The results suggest that in *C. elegans* silica NPs promote a cascade of events including disturbance of protein homeostasis, widespread protein aggregation and inhibition of serotonergic neurotransmission which can be interrupted by compounds preventing amyloid fibrillation.

Keywords

Aging, neurodegenerative disease, neurotoxicology, prevention, proteomics

History

Received 11 May 2015
Revised 3 July 2015
Accepted 13 July 2015
Published online 21 September 2015

Introduction

Current advances and applications of nanotechnology naturally account for a wider distribution of nanoparticles (NPs). Likewise, interactions between nanomaterials and organisms are interesting for both biomedical applications and nanosafety considerations. We study the nematode *Caenorhabditis elegans* to identify the bio-effects of NPs from the molecular via the cellular to the behavioral level.

Caenorhabditis elegans is a real-life model organism that lives in the solid to liquid phase of rotting plant material as part of the soil's food chain. The genome of the nematode was sequenced in the year 1998 (*C. elegans* Sequencing Consortium, 1998). Approximately 20.000 genes encode for the nematode's proteins and the majority of human genes (60–80%) including disease genes have a counterpart/homologue in the worm (Kaletta & Hengartner, 2006). Adult hermaphrodite *C. elegans* invariantly consist of 959 cells of which 302 are neurons. Neural circuits have been mapped that may consist of just a few muscle and neural cells. However, these simple neural circuits drive complex neuromuscular behaviors, e.g. two hermaphrodite-specific motor neurons (HSNs) decisively control egg laying (Zhang et al., 2008). *C. elegans* is transparent which enables imaging of labeled compounds including reporter proteins in single neural cells of living worms. The ease of worm cultivation in solid or liquid culture additionally makes *C. elegans* amenable to biochemical methods and medium to high throughput screening.

Consistent with this state of the art *C. elegans* methods find their application in nanosafety research. High throughput screening has recently been developed for nanotoxicological analyses (Jung et al., 2015). This is extremely valuable in order to keep up with the fast pace of production and application of new nanomaterials. In addition, systems biology analyses have the potential to identify cellular pathways that are affected by NP-interactions in an unbiased manner. Consistently, gas chromatography–mass spectrometry (GC–MS)-based metabolomics showed that titanium dioxide NPs interfere with pathways including the tricarboxylic acid cycle, arachidonic acid metabolism and glyoxalate dicarboxylate metabolism (Ratnasekhar et al., 2015). The reproductive potential (300–350 offspring per worm) and short-life span of adult hermaphrodite *C. elegans* (2–3 weeks) enable investigation of chronic exposures, e.g. the multi-generational as well as life span-resolved characterization of NP-bio-interactions (Contreras et al., 2014; Pluskota et al., 2009).

We previously showed two major uptake pathways of silica NPs via food to the worm's intestine and single intestinal cells or via the vulva to the reproductive system and single vulval cells. Translocation of silica NPs to these target organs induced

Correspondence: Anna von Mikecz, PhD, Professor of Genetics, IUF – Leibniz Research Institute for Environmental Medicine at Heinrich-Heine-University Duesseldorf, Auf'm Hennekamp 50, 40225 Düsseldorf, Germany. Tel: +49 2113389358. E-mail: mikecz@tec-source.de

perturbation of behavioral phenotypes such as reduced pharyngeal pumping and impaired egg laying that are generally age-related. Additionally, an increased propensity for amyloid protein aggregation was identified on a local and global level that likewise support the idea that silica NPs may promote aging in *C. elegans* (Pluskota et al., 2009; Scharf et al., 2013). Based on these results the question arose on how silica-NPs may impact molecular pathways that connect amyloid formation in single cells, a global protein aggregation propensity and impairment of age-associated behavioral phenotypes in an organism. Here, we demonstrate by mass spectrometry-based proteomics that exposure of adult hermaphrodite *C. elegans* with silica NPs induces the segregation of proteins predominately involved in protein homeostasis into an SDS-insoluble aggregome network. As a result widespread protein aggregation is observed that includes the axons of serotonergic HSN neurons. Axonal transport of the neurotransmitter serotonin to the HSN synapse is perturbed which in turn impairs the neuromuscular circuit of egg laying and induces the neural phenotype internal hatch. As protein aggregation in the HSN neuron and internal hatch can be rescued by anti-aging compounds that likewise inhibit amyloid formation we conclude that in *C. elegans* silica NPs cause premature aging by protein homeostasis-driven neurotoxicity.

Materials and methods

Particles

Silica NPs (50 nm diameter, unlabeled or rhodamine-labeled) and BULK silica particles (500 nm diameter; unlabeled) were purchased from Kisker (Steinfurt, Germany). Particles were analyzed by dynamic light scattering in distilled H_2O using the Zetasizer Nano-ZS (Malvern Instruments Ltd., Malvern, United Kingdom) and by live cell imaging as detailed previously (Hemmerich & von Mikecz, 2013; Scharf et al., 2013). The measured mean size (intensity) of unlabeled silica NPs (50 nm), rhodamine-labeled NPs (50 nm) and unlabeled BULK silica particles (500 nm) was 48.65, 45.72 and 445.2 nm in diameter. As measured by laser Doppler electrophoresis the zeta potential of unlabeled silica NPs, rhodamine-labeled NPs and unlabeled BULK silica particles was −60, −53.2 and −66 mV, respectively.

Worm strains, cultivation and particle treatment

C. elegans were cultured at 20 °C under standard conditions on NGM-agar plates supplemented with yeast extract and *Escherichia coli* strain OP50 as food source (Brenner, 1974; Stiernagle, 1999). The following strains were used where indicated: Wild-type N2; AM138 rmIs130 [unc-54 p::Q24::YFP]; AM140 rmIs132 [unc-54 p::Q35::YFP]; AM142 rmIs133 [unc-54 p::Q40::YFP] (Morley et al., 2002); LX975 vsIs13 [pes-10 p::GFP + lin-15(+) IV.], vsIs97 [tph-1 p::DsRed2 + lin-15(+)],vsIs100 [myo-3 p::CFP + lin-15(+)] (Tanis et al., 2008); DR1572 daf-2(e1368) III.; CF1038 daf-16(mu86) I; RW1596 myo-3(st386) V; stEx30 [Pmyo-3::GFP + rol-6(su1006)] (Campagnola et al., 2002). For all experiments, worms were synchronized with hypochlorite/NaOH and cultured on agar plates. One-day-old adults were transferred to fresh NGM-agar or liquid medium in 96-well plates (Petrascheck et al., 2007; Stiernagle, 1999) fed on OP50 supplemented with silica NPs or BULK-silica with a final concentration of 2.5 mg/mL. The latter was titrated as minimal effective concentration concerning reduction of *C. elegans* life span in liquid culture (Piechulek & von Mikecz, unpublished work) and induction of the internal hatch phenotype, reproductive senescence and amyloid protein aggregation on agar plate cultures (Pluskota et al., 2009; Scharf et al., 2013). While environmental concentrations in that range are currently not likely to occur by global proliferation of NPs, materialization of local particle accumulation clusters are thinkable in specific settings (e.g. local leaching of surface coatings, accidental spills and working environments). To maintain worms age-synchronized and to prevent internally hatched larvae, 40 μM FUDR was added to the medium as indicated (Honda et al., 2010).

Mass spectrometry (ESI-LC)

Worms were lysed in SDS-lysis buffer (150 mM NaCl, 10 mM Tris–HCl pH 8, 2% SDS, protease inhibitor) and protein aggregates were isolated via filter retardation assay as described previously (Scharf et al., 2013). Sample preparation, mass spectrometry measurements and data compilation were performed as described previously (Arnhold et al., 2015a). Briefly, SDS-insoluble proteins that were trapped on cellulose acetate membranes were eluted with 6 M guanidinium hydrochloride. After addition of DTT and iodacetamide the samples were dialyzed and digested with trypsin overnight. Dried samples were dissolved in 0.1% formic acid in 5% acetonitrile, cleared by centrifugation and supernatants were used for mass spectrometry analysis in a LTQ Orbitrap XL ETD (Thermo Scientific, Waltham, MA) coupled to a nano-HPLC Nano LC 2D system AS 1 (Eksigent, Dublin, CA). Proteome Discoverer 1.3 (Thermo Scientific, Waltham, MA) was used to process the measured spectra that were searched against the SwissProt database by Mascot (Matrix Science, London, United Kingdom). Data were compiled with Proteome Discoverer 1.3 and Scaffold 3 (Proteome Software, Portland, OR; Arnhold et al., 2015a).

Aggregome analysis: protein classification and structure features

Proteins that were identified in 2 out of 4 biological replicates were subjected to further analysis (Supplementary Tables S1–S3). The identified aggregome candidates were classified according to their biological processes via the PANTHER (Protein ANalysis THrough Evolutionary Relationships) classification system v9.0 (Mi et al., 2013). The PANTHER biological process classification was manually revised with data based on literature, the WormBase (Harris et al., 2014) and the UniProtKB database. The UniProtKB database was also used to extract protein structure features. The percentage of aggregated proteins with beta-sheets was calculated and compared to the total *C. elegans* genome as described previously (Arnhold et al., 2015a).

Microscopy

Living *C. elegans* were analyzed on 5% agarose pads with 10 μM NaN_3 at room temperature. For amyloid-detection worms were fixed via freeze-crack method, stained with 7 mg/mL CongoRed/PBS, mounted in Vectashield (Vector Laboratories, Burlingame, CA) and imaged (Arnhold et al., 2015b; Scharf et al., 2013). Imaging was performed using an epifluorescence/confocal laser scanning microscope (Fluoview, IX70, Olympus, Tokyo, Japan; LSM 510, Zeiss, Oberkochen, Germany) with a 10er/0.3 NA UPlanFl, 40 × /1.3 NA Plan-Neofluar; and a 60 × /1.4 NA Plan Apo objective. Congo red staining and silica NPs were detected with 568 nm excitation/585–640 nm emission, DsRed2 was detected with 561 nm excitation/575–615 nm emission and GFP/YFP was detected with 488 nm excitation/510–550 nm emission.

Quantification of polyQ aggregates

Worms expressing Q35::YFP under the control of the body wall muscle cell-specific promoter *unc-54* (strain AM140) were imaged with a 60 × /1.4 NA Plan Apo objective. Fluorescence quantification analysis was performed with the Metamorph image

analysis software package (Molecular Devices, Sunnyvale, CA) and Microsoft Excel (Redmond, WA). In detail, Q35 aggregates were identified by color threshold (120–255), area threshold (20–300 arbitrary units) and shape factor (>0.4) using the Integrated Morphometry Analysis tool of Metamorph (Molecular Devices, Sunnyvale, CA).

Behavioral assays

Forward locomotion assays were performed as described previously (Hart, 2006). Briefly, synchronized L4 larvae were picked on NGM agar plates supplemented with 40 µM FUDR to avoid internal hatched larvae. One-day-old adult worms were picked and separated on NGM plates supplemented with FUDR and H_2O or silica NPs in the presence of different concentrations of thioflavin T (0.01; 0.1 mM), trehalose (0.1; 1 mM) or ethosuximide (2; 4 mg/mL as indicated. After 24 h body bends were scored for 3 min and the tracks were analyzed. Body bends were defined and quantified as described (Hart, 2006).

For the bag-of-worms-assay (BOW-assay) worms were transferred 90 h post-synchronization into 96-well plates with an average of 15 worms per well. The wells were filled with 150 µL liquid culture medium supplemented with silica NPs or H_2O (mock control) and thioflavin T (0.01 mM), trehalose (0.1 mM), ethosuximide (8 mg/mL), Congo red (0.1 mM). After 26 h worms were analyzed on 5% agar pads and worms that showed internally hatched larvae (moving larvae) were scored as BOW positive.

Pharmacology HSN function assays were performed as described previously (Branicky et al., 2014; Trent et al., 1983). Single worms were transferred to 50 µL M9 supplemented with 10 mg/mL serotonin or 0.75 mg/mL imipramine. The numbers of eggs laid per worm were scored after 90 min.

Statistical analysis

One-way ANOVA with Tukey's post hoc test (Origin 8.5, Origin Lab Corporation, Northampton, MA) or Student's *t* test (Microsoft Excel, Redmond, WA) was used to determine statistical significance. *p* Values below 0.05 were considered as significant.

Results

We previously showed that silica NPs induce a premature accumulation of a SDS-insoluble protein fraction that is otherwise a hallmark of old worms (David et al., 2010; Scharf et al., 2013). As impaired protein homeostasis manifests in fibrillation of generally soluble proteins to intracellular amyloid, untreated or silica NP-exposed worms were imaged with the amyloid-specific dye Congo red by confocal microscopy. As early as 24 h after silica NP-exposure we observed specific binding of Congo red to microenvironments in the cell nucleus, e.g. to the nucleoli of the anteriormost intestinal cells of adult *C. elegans*, indicating formation of amyloid-like nucleolar structures (Figure 1A, middle). Consistent with a NP-specific effect such nucleolar amyloid was neither observable after the mock treatment with H_2O nor the exposure of the worms to BULK silica particles (Figure 1A, left and right, respectively). Silica NP-induced amyloid formation in nucleoli suggests that endogenous nucle(o-l)ar proteins undergo protein fibrillation which is consistent with previous results showing that (i) NPs promote amyloid fibrillation of otherwise soluble proteins *in vitro* by increasing the local protein concentration and nucleation on their surface (Cabaleiro-Lago et al., 2012; Linse et al., 2007) and (ii) amyloid-like nuclear protein aggregation in mammalian cell culture after silica NP- or inorganic mercury exposures (Arnhold & von Mikecz, 2011; Arnhold et al., 2015a; Chen et al., 2008).

Next we analyzed, if silica NPs exclusively induce protein aggregation in intestinal cells or likewise in other tissues. To this end transgenic worms that stably express a homopolymeric repeat of 35 glutamines fused to yellow fluorescent protein (Q35::YFP) in the body wall muscle cells (Morley et al., 2002) were left untreated (H_2O) or exposed to silica NPs for 24 h. Untreated worms express the reporter protein throughout the body wall muscle cells which results in a smooth continuous staining pattern (Figure 1B, top), whereas the silica NP-exposed *C. elegans* display a discontinuous, dotted staining indicating aggregation of Q35::YFP (Figure 1B, bottom). The corresponding quantification shows that the change from a continuous to a dotted, e.g. protein aggregate staining pattern is significant (Figure 1C). Similar aggregation of proteins with polyglutamine(polyQ) repeats

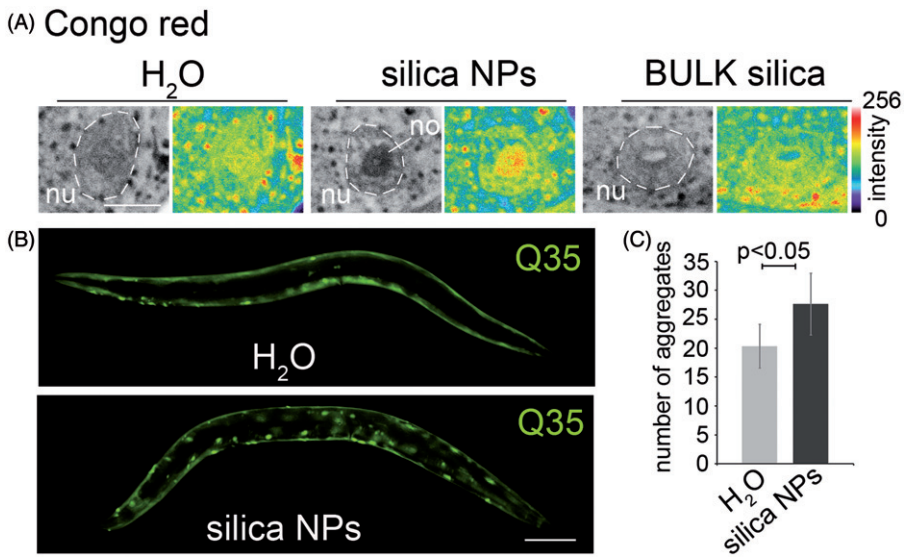

Figure 1. Silica NPs induce widespread protein aggregation in adult *C. elegans*. (A) Representative fluorescent micrographs of the anterior-most intestinal cell nuclei of 2-day-old, adult *C. elegans* (N2, wild type). Worms were mock(H_2O)-treated or exposed to silica NPs or BULK silica in liquid culture for 24 h, fixed and stained with the amyloid-specific dye Congo red. Congo red is shown as inverted greyscale and in pseudocolor as intensity maps. Blue indicates low intensity, whereas red indicates high intensity of the staining. Bar, 7.5 µm. (B) Representative fluorescent micrographs of 2-day-old, adult *C. elegans* stably expressing a homopolymeric glutamine repeat fused to yellow fluorescent protein (Q35::YFP) under the control of the *unc-54* promoter in the body wall muscle cells. Worms were mock-treated or exposed to silica NPs in liquid culture for 24 hours. Bar, 100 µm. (C) Respective quantification of the number of Q35::YFP aggregates per worm. Values represent means ± SD of four independent experiments with $n > 150$ for each treatment (H_2O versus silica NPs, Student's *t* test $p < 0.05$). No, nucleolus; nu, nucleus; Q35, homopolymeric repeat of 35 glutamines fused to yellow fluorescent protein. The online version contains colored figures.

typically occurs in neurodegenerative diseases such as Huntington's disease (HD) and certain ataxias. In HD nuclear inclusions consisting of polyQ repeat proteins characteristically occur in distinct brain regions, e.g. cortical neurons. The underlying mechanism of protein aggregation is studied in *C. elegans* disease models where polyQ stretches of different length are expressed by fusion with reporter genes such as YFP (Brignull et al., 2006). Notably, the excess of a critical threshold of polyQ repeat length (Q40 and above) correlates with amyloid-like protein aggregation in worms and patients (Klein et al., 2007). Here, we show that in respective *C. elegans* polyQ disease models silica NPs reduce this threshold from Q40 to Q35 and apparently act as enhancers of widespread protein aggregation in a living organism (Figure 1B and C; Supplementary Figure S1, right column).

Silica NPs accelerate fibrillation of proteins to an SDS-insoluble aggregome

In order to identify the cellular pathways of silica NP-induced amyloid formation all endogenous proteins that segregate into an insoluble SDS-resistant protein fraction were characterized by mass spectroscopy (MS). Wild-type adult *C. elegans* were left untreated or exposed to silica NPs for 24 hours and lysed. Insoluble proteins were purified by means of a filter retardation assay that traps SDS-resistant protein aggregates on a cellulose acetate filter, while allowing soluble proteins to pass through the 0.2 µm sized pores (Figure 2A; Scherzinger et al., 1997). In order to distinguish single components of a silica-NP-induced aggregome the trapped protein fraction was eluted from the filters and subjected to MS as detailed in the Methods section (Figure 2A).

MS allows for an unbiased analysis of the aggregome network that fibrillates after silica NP-exposure. In mock(H_2O)-treated control worms this aggregome consists of 73 candidate proteins,

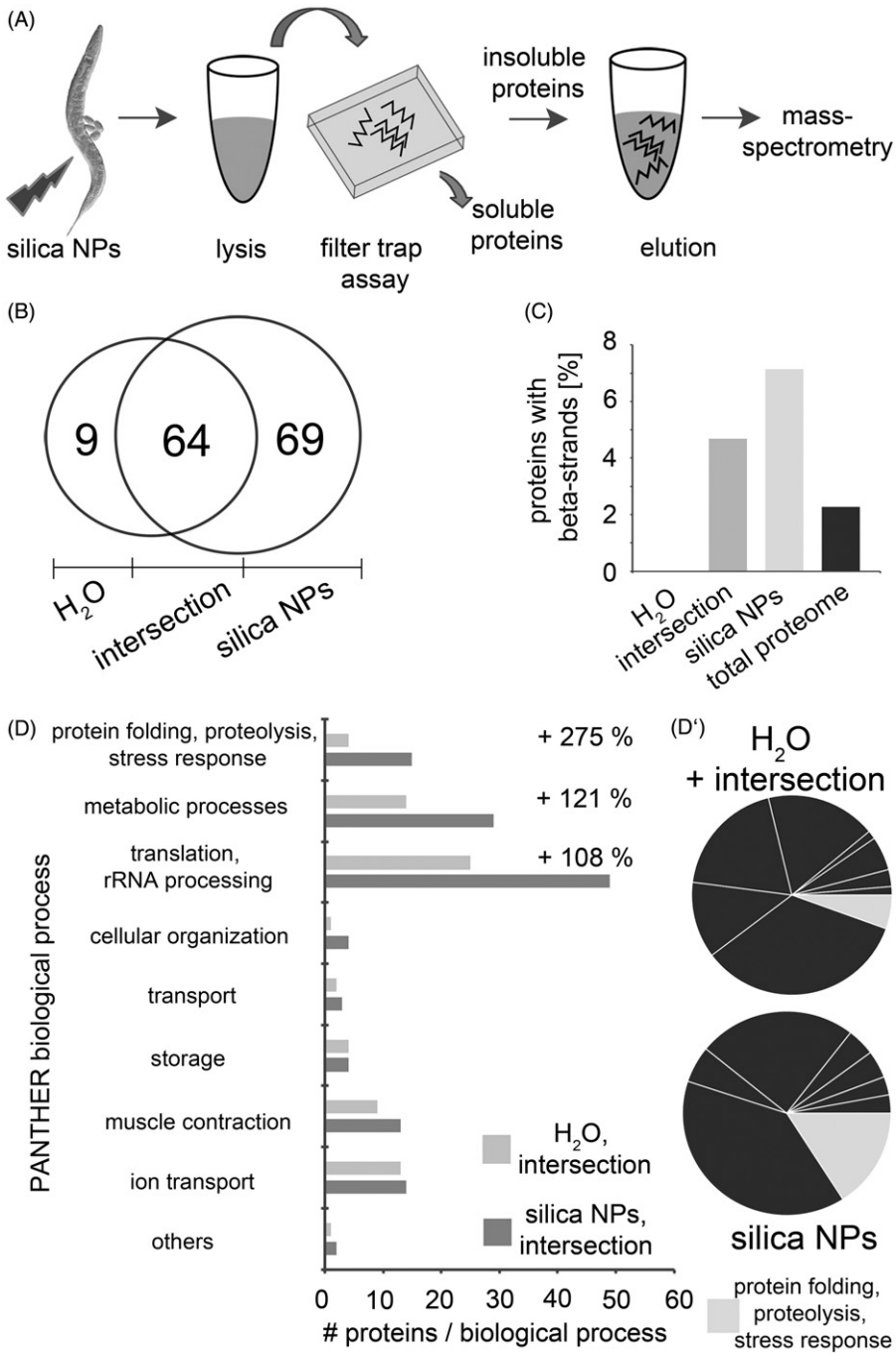

Figure 2. Silica NPs accelerate fibrillation of proteins to a SDS-insoluble aggregome. (A) Schematic of the purification and mass spectrometry (MS) of SDS-insoluble protein aggregates: *C. elegans* were left untreated (H_2O) or exposed to silica NPs for 24 h and lysed. SDS-insoluble proteins were isolated via filter trap assays, eluted with 6 M guanidinium hydrochloride and analyzed by mass-spectrometry (ESI-LC/MS). (B) Venn diagram of the MS results. (C) Analysis of the structural features of the aggregated proteins based on the UniProtKB database. The graph shows the percentage of aggregated proteins with beta-sheets compared to the total *C. elegans* genome. (D) GO analysis of the aggregome networks. Candidate proteins are grouped according to biological processes as classified by the PANTHER database (Mi et al., 2013). The classification was revised using current literature and the WormBase. The bar graph compares the absolute numbers of the identified aggregated proteins in the H_2O- versus silica NP-induced aggregome including respective intersections. The percentage represents the change of each functional group in the control (H_2O) versus the silica NP-induced aggregome. (D') A pie chart illustrates the increase of the GO group of ''protein folding, proteolysis and stress response'' in the silica NP-induced aggregome.

whereas 69 proteins specifically segregate into a silica NP-induced aggregome network (Figure 2B; Supplementary Tables S1–S3). Analysis of the proteomic data revealed that the silica NP-specific aggregome is enriched in proteins containing beta-strand structures in comparison with the total proteome (Figure 2C). This is consistent with the notion that beta-strands possess an intrinsic propensity for amyloid protein fibrillation (Neudecker et al., 2012). Next, the function of the aggregome components was investigated by a GO analysis (Figure 2D). Using the PANTHER database (Mi et al., 2013) GO groups were identified that show significant changes after silica NP-exposure. With 275% the GO group of ''protein folding, proteolysis and stress response'' accounts for the largest silica NP-specific increase suggesting that respective proteins segregate to an SDS-resistant aggregome network due to the exposure of the worms to the nanomaterial (Figure 2D and D′). Candidate proteins in this group include chaperones, heat shock proteins, subunits of the 26S proteasome and the nascent polypeptide-associated complex subunit alpha that are all involved in different aspects of protein homeostasis (Supplementary Table S3). Their segregation into an SDS-insoluble aggregome network corroborates the idea that silica NPs promote widespread protein aggregation by fuelling a vicious circle. Proteins involved in protein homeostasis undergo amyloid fibrillation themselves, are inactivated by segregation in amyloid-like microenvironments and thus enhance further fibrillation of other proteins. Consistently, immunoblot analyses indicated that proteasomes are equally expressed in untreated control worms and silica NP-exposed worms, e.g. are not depleted from the total proteome, but rather segregate into amyloid microenvironments (Supplementary Figure S2). Such segregation of ubiquitin-proteasome system components was previously observed in mammalian cell culture (Arnhold et al., 2015a; Chen et al., 2008) and represents a hallmark of neural nuclear inclusions in neurodegenerative protein aggregation diseases such as amyotrophic lateral sclerosis, Parkinson's or HD) diseases (Ross & Poirier, 2004).

Further GO groups containing at least 10 candidates that were specifically increased by silica NPs include ''metabolic processes'' (121%) as well as ''translation and ribosomal RNA (rRNA) processing'' (108%; Figure 2D). Notably, ''translation and rRNA processing'' represents the largest GO group with a total of 49 candidate proteins. As rRNA synthesis and processing as well as ribosome assembly occurs in the nucleolus the proteomic data validate our Congo red-based imaging results that located amyloid fibrillation in single nucleoli of silica NP-exposed *C. elegans* (Figure 1A). Taken together, the imaging and MS results suggest that the nucleolus is a major target of amyloid fibrillation and may contain a substantial fraction of the silica NP-induced aggregome network.

Behavioral phenotyping validates protein homeostasis as the major pathway of silica-NP-bio-interactions

As the GO group of ''protein folding, proteolysis and stress response'' showed the largest increase (275%) of aggregome components after silica NP-induction it was further analysed by behavioral phenotyping. To this end neuromuscular behaviors such as locomotion and egg laying were investigated concerning their sensitivity to silica NPs and the rescue of potential defects by inhibitors of amyloid protein aggregation. Worms that were treated with silica NPs exclusively altered their locomotory pattern from carving regular sinusoidal tracks into agar plates to a serrated forward locomotion pattern (Figure 3A and A′). Additionally, they moved with reduced speed in comparison to untreated control animals or worms that were exposed to BULK silica particles (Supplementary Videos S1–S3). A quantification of body bends revealed that untreated worms performed about 17 bends per minute, whereas silica NPs reduced this locomotion phenotype to 8–13 bends/min (Figure 3B–D). Notably, such reduction was in turn reversed by co-incubation with increasing concentrations of compounds that inhibit amyloid formation such as ethosuximide, thioflavin T, Congo red or trehalose (Figure 3B–D) (Alavez et al., 2011; Chen & von Mikecz, 2005; Chen et al., 2008; Evason et al., 2005; Frid et al., 2007; Honda et al., 2010; Tanaka et al., 2004). These compounds share the property to reduce amyloid formation, ameliorate symptoms in animal models of neurodegenerative diseases (Alavez et al., 2011; Frid et al., 2007; Tanaka et al., 2004) and prolong the life span of *C. elegans* (Alavez et al., 2011; Honda et al., 2010) suggesting a close relationship between silica NP-induced alteration of protein homeostasis, defective behavioral phenotypes and organismal aging processes.

While the neuromuscular circuits regulating locomotion are largely unknown, the egg laying phenotype is specific for adult hermaphrodite *C. elegans* and based on a well-defined neural circuit driven by two serotonergic HSN motor neurons (Zhang et al., 2008). Thus, we investigated the effects of silica NP-induced impairment of protein homeostasis on egg laying and the potential rescue of worm behavior by inhibitors of amyloid protein aggregation. Exposure of wild type worms with silica NPs for 26 h resulted in a significant increase ($p < 0.01$) of the egg laying defect internal hatch/BOW that generally occurs in aged worms or certain mutant strains (Figure 3E; Schafer, 2006). Due to a malfunction of the vulva eggs are not laid and the young worms hatch within the parent's body. In contrast to the effects of the silica NP-exposure (72% BOW), mock(H_2O)-treated controls or worms exposed to BULK silica showed a regular number of animals with internal hatch, e.g. 9% or 14% BOW, respectively (Figure 3E). Co-incubation of worms with silica NPs and the inhibitors of amyloid formation ethosuximide, thioflavin T, trehalose or Congo red rescued the nanomaterial-effect and reduced the BOW phenotype (between 11% and 53%; Figure 3E). While ethosuximide ($p < 0.01$), thioflavin T ($p < 0.05$) and Congo red ($p < 0.01$) significantly reduced internal hatch to levels comparable with untreated control worms, trehalose rescued the silica NP-induced BOW to 53%, however, not significantly, due to a substantial standard deviation (Figure 3E).

As ethosuximide also represents a well-defined anti-aging compound that significantly prolongs the life span of adult *C. elegans* (Evason et al., 2005) worm strains with mutations in the insulin signaling pathway that either prolong life span (*daf-2*) or reduce life span (*daf-16*) were left untreated or exposed to silica NPs. Notably, a significant induction of the BOW phenotype was observed in wild type worms ($p < 0.01$) as well as in *daf-2* ($p < 0.01$) and *daf-16* ($p < 0.01$) mutants suggesting that the insulin signalling pathway is not targeted by silica NP-bio-interactions (Figure 3F). This is consistent with the absence of insulin pathway components from the silica NP-induced aggregome (Supplementary Table S3).

Based on the behavioral phenotyping analyses, we conclude that silica NPs interact with aging pathways involving protein homeostasis and amyloid protein aggregation, however independently from insulin signalling. This validates our results obtained by MS that indicated the GO group ''protein folding, proteolysis and stress response'' as a major target of silica NP-effects. We introduce behavioral phenotyping in *C. elegans* as a tool to validate the proteomic results and identify the relevant cellular pathways.

Protein aggregation occurring in dendrites of HSN neurons disrupts axonal transport and promotes neurotoxicity

Next, we wanted to know how a silica NP-induced aggregome network that segregates components of the protein homeostasis

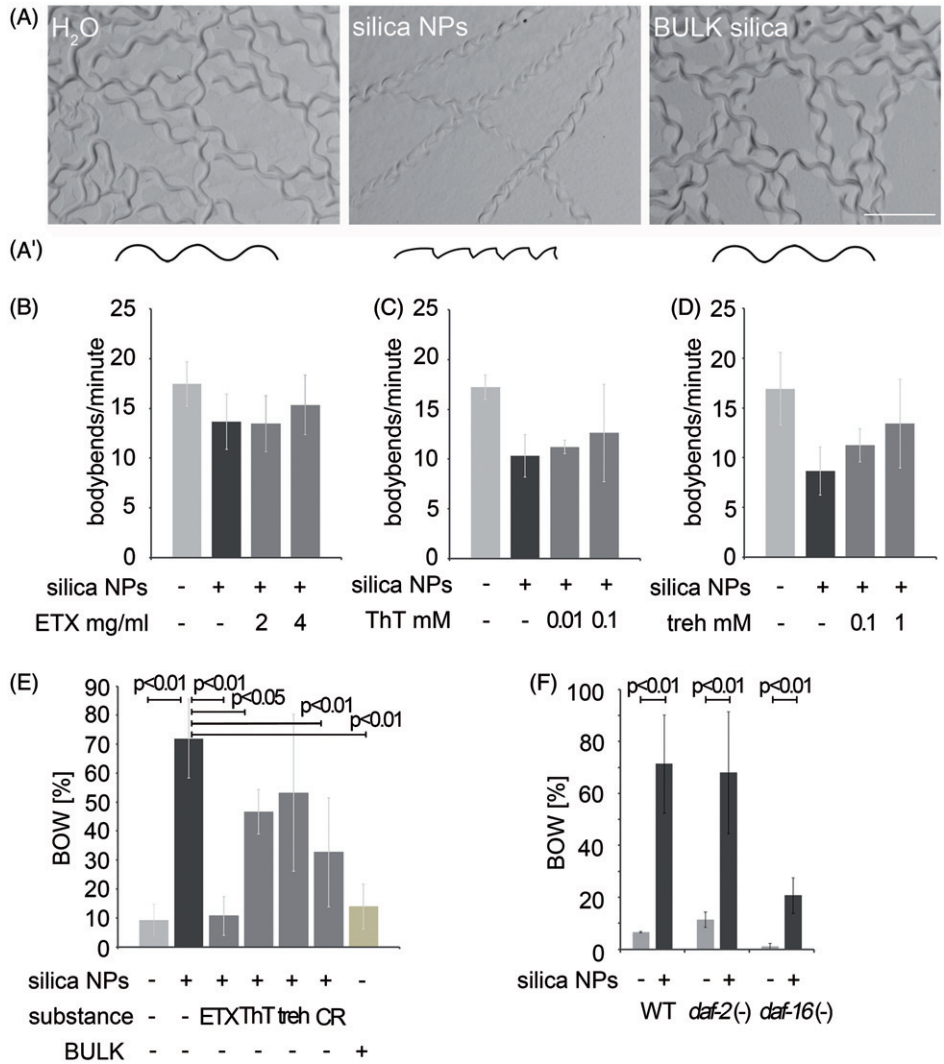

Figure 3. Cellular pathway validation by behavioral phenotyping. (A) Micrography of representative forward locomotion tracks on agar plates of 2-day-old, adult wild type *C. elegans* that were mock (H_2O)-treated or exposed to silica NP, or BULK silica for 24 h (A′) Schematic of the tracks showing that the H_2O- and BULK silica-treated worms crawl in sinusoidal curves, whereas silica NP-treated worms move in a serrated pattern. (B–D) Quantification of the locomotion by body bend counts per minute of 2-day-old, adult wild type *C. elegans* that were treated with H_2O, silica NPs or silica NPs in combination with different concentrations of inhibitors of amyloid formation for 24 h: (B) ethosuximide, (C) thioflavin T and (D) trehalose. Values represent means ± SD from four independent experiments with $n \geq 17$ for each treatment. (E) Ratio of the internal hatch/bag of worms (BOW) phenotype in a population of 2-day-old, adult wild type *C. elegans* that were treated for 26 h with H_2O, silica NPs, BULK silica or silica NPs in combination with ethosuximide, thioflavin T, Congo red or trehalose in liquid medium. Silica NP-treated worms show an increase of the BOW-phenotype that is fully rescued by ethosuximide. Values represent means ± SD from at least three independent experiments with $n > 100$ for each treatment (H_2O; ethosuximide/silica NPs; Congo red/silica NPs; BULK silica versus silica NPs, one-way ANOVA with Tukey's post hoc test $p < 0.01$; thioflavin T/silica NPs versus silica NPs, one-way ANOVA with Tukey's post hoc test $p < 0.05$). (F) Ratio of the BOW-phenotype in a population of 2-day-old, adult wild type *C. elegans* compared with long-lived *daf-2* mutants or short-lived *daf-16* mutants that were treated for 26 h with H_2O, silica NPs. Values represent means ± SD from four independent experiments with $n > 170$ for each genotype and treatment (H_2O versus silica NPs, one-way ANOVA with Tukey's post hoc test $p < 0.01$). BOW, bag of worms; CR, Congo red; ETX, ethosuximide; ThT, thioflavin T; treh, trehalose.

pathway may affect a complex *C. elegans* behavior such as egg laying. In *C. elegans,* the egg laying organ, e.g. the vulva, consists of a straightforward number of seven vulval cells (vulA, B1, B2, C, D, E and F), two vulval muscles (vm1L/R and vm2L/R) and eight egg laying neurons (VC1-6, HSNL/R; Figure 4(A) and (B); schematics). Ablation analyses revealed that the HSN motor neurons decisively control the egg laying behavior (Lints & Hall, 2009; Zhang et al., 2008).

To investigate if silica NPs affect the morphology of the egg laying organ worms that stably express a myosin3::green fluorescent protein (Pmyo3::GFP) reporter were exposed to the respective particles for 48 h. Representative micrographs show that labeled silica NPs translocate into vulval cells, especially vulD, vulE and vulF (Figure 4B and B′; red color). This confirms previous observations of a silica NP-burden occurring in single vulval cells (Scharf et al., 2013). The silica NP-exposure did not induce any changes of the characteristic x-shaped morphology of intact vulval muscles (Figure 4B and B′; green color; schematics; Lints & Hall, 2009). Consistently, the myosin filaments in body wall muscle cells of silica NP-treated myo3-reporter worms are organized into a continuous sarcomere banding pattern (Supplementary Figure S3).

As suggested by their intact morphology, vulval muscles are not a target for silica NP-bio-interactions. Thus, we next analyzed the functionality of the muscles within the neuromuscular egg laying circuit. To this end a ''drug egg laying assay'' was performed (Branicky et al., 2014). The assay is based on the exogenous gavage of the neurotransmitter serotonin which

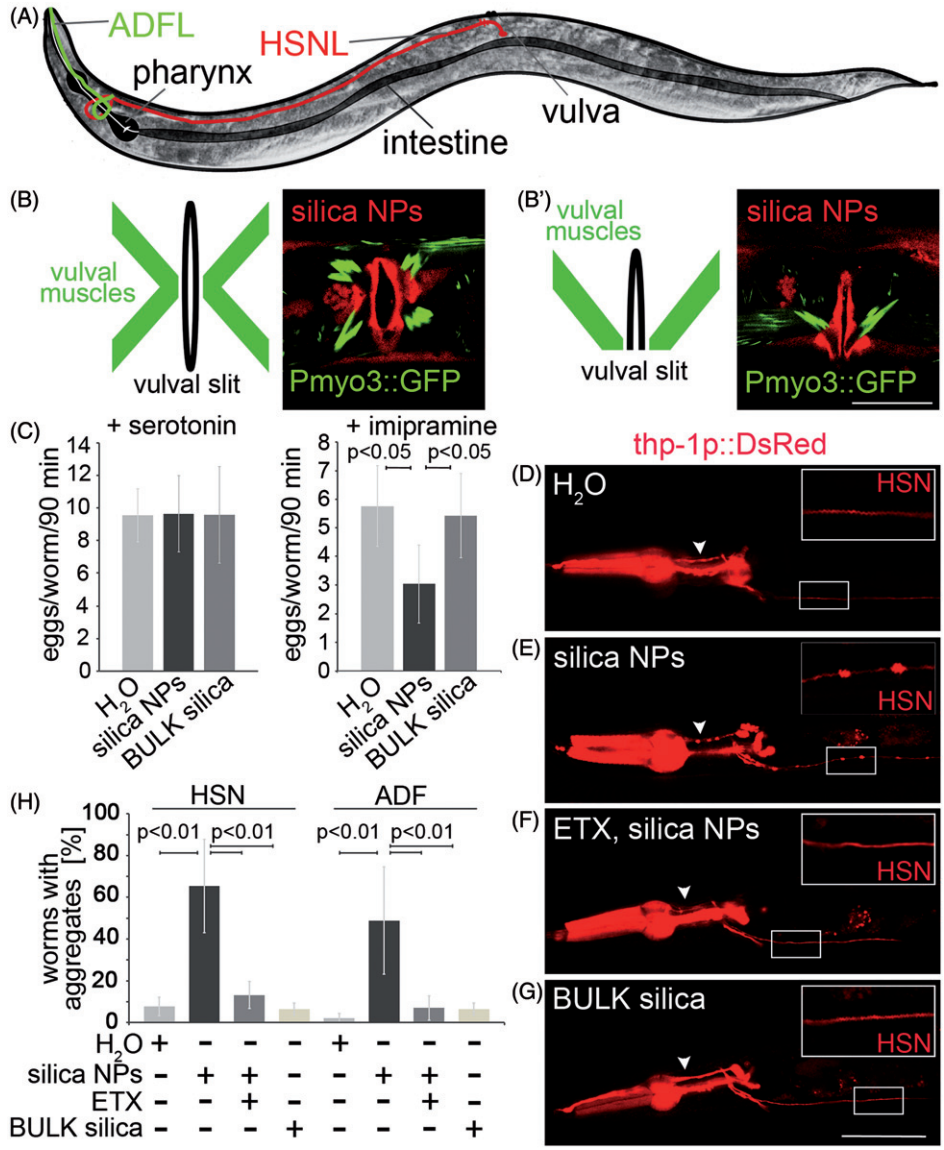

Figure 4. Silica NPs induce neurodegeneration. (A) Schematic of an adult hermaphrodite worm depicting the serotonergic neurons HSNL (red) and ADFL (green; Hall et al., 2006). The cell body of the HSNL localizes posterior to the vulva, whereas the axon runs along the posterior–anterior axis and extends into the nerve ring of the pharynx. Schematic ventral (B) and lateral (B′) view of the adult hermaphrodite egg-laying organ including the vulval muscles and the vulval cells (vulval slit; Lints & Hall, 2009). (B, B′) Respective fluorescent micrographs of representative 3-day-old, adult worms stably expressing green fluorescent protein (GFP) under the control of the myosin-3 (myo-3) promoter that were treated with rhodamine-labeled silica NPs for 48 h. Rhodamine-labeled silica NPs translocate into single vulva-cells vulF, vulE and vulD (red color). Vulval muscles show an intact morphology (green color). Bar, 10 µm. (C) Pharmacology assay of HSN function (Branicky et al., 2014). The graph illustrates the number of eggs that are laid per 3-day-old, adult wild type hermaphrodite worm exposed to exogenous serotonin or imipramine. Vulval muscle stimulation by exogenous serotonin induces similar egg laying behavior of mock (H_2O-), silica NP- or BULK silica-treated worms indicating intact muscles. The serotonin-reuptake inhibitor imipramine shows significantly reduced egg laying in silica NP-exposed (48 h) worms compared to the controls (mock- or BULK silica-treated worms) indicating a reduced availability of endogenous serotonin at the synapse, e.g. a defect in HSN function. Values represent means ± SD from at least three independent experiments, $n \geq 70$ for each treatment. (D–G) Representative fluorescent micrographs of 2-day-old, adult *C. elegans* stably expressing DsRed2 under the control of the tryptophan hydroxylase (*tph-1*) promoter in serotonergic neurons that were treated for 24 h with either (D) H_2O (mock control), (E) silica NPs, (F) a combination of silica NPs with 4 mg/mL ethosuximide or (G) BULK silica in liquid culture. The insets show blow-ups of the HSN axon. Silica NP-treated worms exhibit aggregated DsRed along the HSN axons (insets) as well as along the ADF axons (arrowhead). Worms that are treated with a combination of silica NPs and ethosuximide show a continuous fluorescence along the axons similar to the control worms (H_2O or BULK). Bar, 50 µm. (H) Respective quantification of worms with DsRed2 aggregates along the HSN and the ADF axons. Values represent means ± SD from four independent experiments, $n \geq 78$ (H_2O, silica NPs/ethosuximide or BULK silica versus silica NPs; one-way ANOVA with Tukey's post hoc test $p < 0.01$). ETX, ethosuximide. The online version contains colored figures.

induces neurotransmission between the HSN neuron and vulval muscles, thereby activating the egg laying phenotype within a defined time window. Consistent with the idea that vulval muscles remain functional it was shown that untreated (H_2O), silica NP-treated and BULK silica-exposed hermaphrodite *C. elegans* laid similar numbers of eggs (9–10) within 90 min if egg laying was stimulated by exogenous serotonin (Figure 4C, left). Notably, imipramine that inhibits serotonin reuptake from the synaptic cleft and thereby generally prolongs serotonergic neurotransmission did stimulate egg laying in H_2O-and BULK silica-treated control worms (5 eggs/worm/90 min), however, with significantly reduced efficiency in silica NP-exposed worms (3 eggs/worm/90 minutes; Figure 4C, right). The significant inability of the reuptake inhibitor imipramine to stimulate serotonergic

neurotransmission in silica NP-treated worms indicates a reduced availability of endogenous serotonin in the synaptic cleft, e.g. impairment of HSN function.

The morphological analyses as well as serotonin-stimulated egg laying tests confirmed that vulval muscles remain functional after exposure of worms to silica NPs. The results rather pointed to neural transmission and neurotoxicity as targets of silica NP-bio-interactions. We therefore investigated the serotonergic HSN motor neurons that decisively control egg laying (Zhang et al., 2008) in more detail. To this end worms that stably express the reporter protein DsRed2 under the control of the tryptophan hydroxylase (*tph-1*) promoter in the serotonergic neurons HSN and ADF (Tanis et al., 2008) were left untreated (H_2O) or exposed to silica NPs or BULK silica (Figure 4A and D–G). While the control worms (H_2O or BULK silica) displayed a distinct continuous staining pattern of the neural soma and dendrites (Figure 4D and G; insets), a punctated, disrupted staining of DsRed was observable along the axons of HSN (Figure 4E, inset) as well as ADF (Figure 4E, arrowhead) neurons in silica NP-treated worms. The DsRed puncta occur distinctly spaced throughout the HSN axon like beads on a string indicating silica NP-induced protein aggregation and presynaptic accumulation of the reporter protein DsRed. While DsRed is known to form tetramers (Pakhomov & Martynov, 2008) the size of the puncta along the HSN axon rather resemble previous observations describing neurotoxin-induced presynaptic protein aggregation of the dopamine transporter (Nass et al., 2002) and axonal disruptions (Fatouros et al., 2012) in *C. elegans*.

To confirm that the puncta on the HSN axons indeed represent protein aggregates DsRed reporter worms were co-incubated with silica NPs and ethosuximide (Figure 4F and H). The addition of ethosuximide prevented the silica NP-induced aggregation pattern in the HSN neurons, e.g. presynaptic accumulation of DsRed along the HSN axon, suggesting that silica NPs impair the physiological interactions between protein homeostasis, neural function and worm behavior.

Discussion

Taken together the results show that silica NPs initiate a cascade of events that starts with widespread protein aggregation. Intracellular amyloid formation segregates endogenous proteins with essential roles in maintenance of protein homeostasis into an aggregome network, thus reducing their functionality and fueling further protein aggregation (Figures 1 and 2). Such protein aggregation likewise occurs in axons of HSN neurons, where presynaptic accumulation of serotonin, e.g. disturbed axonal transport, reduces the capacity for neurotransmission (Figure 4). In turn, the impairment of neural function may cause the apparent defects in neural behaviors that are observed after exposure of adult *C. elegans* to silica NPs. Consistent with this idea inhibitors of amyloid aggregation significantly reduce the neural behavior defects initiated by silica NPs (Figure 3).

Thus, silica NPs promote neurotoxicity targeting serotonergic neurons in a real life organism. On the single-cell level we identify protein aggregation in axons of HSN neurons that is closely involved with impairment of its neural function, e.g. the worm's egg laying behavior. These NP-specific effects are preventable by compounds that inhibit amyloid formation and likewise prolong the life span of adult *C. elegans* (Alavez et al., 2011; Honda et al., 2010). Due to the proven similarities between the nervous systems of *C. elegans* and mammals concerning the workings of serotonergic neurotransmission our results offer mechanistic insights into how and where silica NPs may interact if they come in contact to the respective tissues and organs. Consistent with this it is noteworthy that the observed amyloid protein aggregation occurs in (i) cells with visible intracellular uptake of silica NPs, e.g. intestinal and vulval epithelium (Scharf et al., 2013), (ii) sensory ADF amphid neurons with direct contact to the environment or (iii) HSN neurons that have an as yet unknown status concerning intracellular localization of NPs. As a deeper penetration of silica NPs into pharyngeal tissue was demonstrated by light sheet microscopy (Scharf et al., 2013), NP-uptake into HSN neurons is conceivable. Further super resolution imaging and coherent anti-Stokes Raman scattering techniques have the potential to clarify the correlation between localization of nanomaterials and their organismal effects, including neural function, in more detail.

Notably, silica NPs promote neurodegeneration in *C. elegans* that is otherwise observed in neurodegenerative aggregation diseases such as HD. Disturbance of axonal transport, e.g. traffic, was identified as a target of the pathology in HD patients and respective *Drosophila* and murine animal models (Feany & La Spada, 2003; Gunawardena et al., 2003; Li et al., 2001). Axonal aggregation of huntingtin in HD mice impaired axonal transport and lead to the degeneration of the respective neurons (Li et al., 2001). Likewise disturbance of the serotonin transport by NP-induced widespread protein aggregation may lower the availability of the neurotransmitter within the synaptic cleft to a threshold low that does not allow further HSN functionality. Consistent with this idea it has been shown that already small changes in serotonin levels critically impact worm behavior (Tanis et al., 2008). In addition to disrupted neural circuitry it was demonstrated that mitochondrial dysfunction plays a role in HD-associated neurodegeneration (Labbadia & Morimoto, 2013). Notably, mitochondrial proteins are overrepresented in the silica NP-specific aggregome indicating that mitochondrial function might likewise represent a target in *C. elegans* and contribute to silica NP-induced neurodegeneration.

While unbiased proteomics and single cell *in vivo* imaging clearly identify the pathway of protein homeostasis as a major molecular target of silica NPs and intracellular amyloid formation as a consequence in *C. elegans*, it is unknown if nanomaterials may reach the peripheral as well as central nervous systems of higher organisms. The olfactory bulb has been identified as an entry portal for trace metals and certain NPs to the central nervous system of mammals (Lucchini et al., 2012). However, the relevance of such an exposition for silica nanomaterials is currently unclear and under investigation.

In this study, neurotoxic outcomes of silica NPs in adult *C. elegans* were broken down to single serotonergic neural cells (HSN), facilitation of protein aggregation in axons and disturbed neurotransmission. Molecular pathways that were identified by proteomics were validated by behavioral phenotyping using inhibitors of the respective pathways. We suggest the application of these methods for further investigation of age-resolved effects of NPs on the worm's neural system. Recently, it was shown that the nervous system of adult *C. elegans* ages and aging neurons develop extra neurite branches (Tank et al., 2011). Such phenotypes together with other typical aging phenotypes, e.g. internal hatch/BOW, represent a promising approach to investigate the effects of chronic NP-exposures (Scharf et al., 2013). Interestingly, degeneration of neural phenotypes through silica NPs is independent of insulin signaling (this study), whereas the insulin/IGF-1 pathway affects the age-related neurite branching (Tank et al., 2011) suggesting that silica nanomaterials may accelerate organismal aging processes without usage of the conventional signaling pathways.

While our results of the reuptake inhibitor imipramine and presynaptic DsRed accumulation suggest a scenario of reduced serotonin levels at the synapse due to impaired axonal transport, one should not forget that a major GO group of the silica NP-

induced aggregome network is ''translation and rRNA processing'' (Figure 3; Supplementary Table S3). Thus, ribosome biogenesis in the nucleolus, rRNA processing as well as translation are likewise targets of silica NP-bio-interactions and require further investigation, especially with respect to peculiar effects on neuronal function, e.g. neurodegeneration. A general reduction of translation by silica NPs, however, can be excluded due to the equal gene expression that was observed in the total, soluble protein fraction of untreated versus nanomaterial exposed worms (Scharf et al., 2013; Supplementary Figure S2, input).

Conclusions

Our study identifies neurotoxic effects of silica NPs *in vivo*, e.g. in the soil nematode *C. elegans*, that are caused by accelerated amyloid protein aggregation. In adult hermaphrodite worms impairment of serotonergic neurotransmission results in silica NP-induced neuromuscular defects of the egg laying apparatus. These defects are in turn reducible by anti-amyloid compounds. We suggest that silica NP-induced axonal disturbance of the HSN motor neuron in combination with the HSN-controlled behavioral defect of internal hatch (BOW) may serve as (i) a model system to further investigate the interactions between amyloid aggregation, axonal transport and neurodegeneration as well as (ii) a screening tool to identify compounds that prevent this neurodegeneration cascade. At the same time, the HSN/BOW *C. elegans* model of NP-bio-interactions may serve as a platform to develop standardized medium and high throughput screening protocols for the definition of neuro-safe nanomaterials.

Acknowledgements

We thank Florian Arnhold (posthumous) for help with the proteome analyses. We likewise thank WormBase. Some strains were provided by the *Caenorhabditis elegans* Center (CGC), which is funded by the NIH Office of Research Infrastructure Programs (P40 OD010440). We gratefully acknowledge the kind support of Stefanie Weidtkamp-Peters at the Center for Advanced Imaging (CAI, Heinrich-Heine-University Duesseldorf).

Declaration of interest

The authors declare no conflicts of interest.

References

Alavez S, Vantipalli MC, Zucker DJ, Klang IM, Lithgow GJ. 2011. Amyloid-binding compounds maintain protein homeostasis during ageing and extend lifespan. Nature 472:226–9.

Arnhold F, Gührs KH, von Mikecz A. 2015a. Amyloid domains in the cell nucleus controlled by nucleoskeletal protein lamin B1 reveal a new pathway of mercury neurotoxicity. Peer J 3:e754.

Arnhold F, Scharf A, von Mikecz A. 2015b. Imaging and quantification of amyloid fibrillation in the cell nucleus. Methods Mol Biol 1228: 187–202.

Arnhold F, von Mikecz A. 2011. Quantitative feature extraction reveals the status quo of protein fibrillation in the cell nucleus. Integr Biol (Camb) 3:761–9.

Branicky R, Miyazaki H, Strange K, Schafer WR. 2014. The voltage-gated anion channels encoded by clh-3 regulate egg laying in *C. elegans* by modulating motor neuron excitability. J Neurosci 34: 764–75.

Brenner S. 1974. The genetics of *Caenorhabditis elegans*. Genetics 77: 71–94.

Brignull HR, Moore FE, Tang SJ, Morimoto RI. 2006. Polyglutamine proteins at the pathogenic threshold display neuron-specific aggregation in a pan-neuronal *Caenorhabditis elegans* model. J Neurosci 26: 7597–606.

Cabaleiro-Lago C, Szczepankiewicz O, Linse S. 2012. The effect of nanoparticles on amyloid aggregation depends on the protein stability and intrinsic aggregation rate. Langmuir 28:1852–7.

Campagnola PJ, Millard AC, Terasaki M, Hoppe PE, Malone CJ, Mohler WA. 2002. Three-dimensional high-resolution second-harmonic generation imaging of endogenous structural proteins in biological tissues. Biophys J 82:493–508.

C. elegans Sequencing Consortium. 1998. Genome sequencing of the nematode *C. elegans*: a platform for investigating biology. Science 282: 2012–18.

Chen M, Singer L, Scharf A, von Mikecz A. 2008. Nuclear polyglutamine-containing protein aggregates as active proteolytic centers. J Cell Biol 180:697–704.

Chen M, von Mikecz A. 2005. Formation of nucleoplasmic protein aggregates impairs nuclear function in response to SiO_2 nanoparticles. Exp Cell Res 305:51–62.

Contreras EQ, Puppala HL, Escalera G, Zhong W, Colvin VL. 2014. Size-dependent impacts of silver nanoparticles on the lifespan, fertility, growth, and locomotion of *Caenorhabditis elegans*. Environ Toxicol Chem 33:2716–23.

David DC, Ollikainen N, Trinidad JC, Cary MP, Burlingame AL, Kenyon C. 2010. Widespread protein aggregation as an inherent part of aging in *C. elegans*. PLoS Biol 8:e1000450.

Evason K, Huang C, Yamben I, Covey DF, Kornfeld K. 2005. Anticonvulsant medications extend worm life-span. Science 307: 258–62.

Fatouros C, Pir GJ, Biernat J, Koushika SP, Mandelkow E, Mandelkow EM, et al. 2012. Inhibition of tau aggregation in a novel *Caenorhabditis elegans* model of tauopathy mitigates proteotoxicity. Hum Mol Genet 21:3587–603.

Feany MB, La Spada AR. 2003. Polyglutamines stop traffic: axonal transport as a common target in neurodegenerative diseases. Neuron 40:1–2.

Frid P, Anisimov SV, Popovic N. 2007. Congo red and protein aggregation in neurodegenerative diseases. Brain Res Rev 53:135–60.

Gunawardena S, Her LS, Brusch RG, Laymon RA, Niesman IR, Gordesky-Gold B, et al. 2003. Disruption of axonal transport by loss of huntingtin or expression of pathogenic polyQ proteins in *Drosophila*. Neuron 40:25–40.

Hall DH, Lints R, Altun Z. 2006. Nematode neurons: anatomy and anatomical methods in *Caenorhabditis elegans*. Int Rev Neurobiol 69: 1–35.

Harris TW, Baran J, Bieri T, Cabunoc A, Chan J, Chen WJ, et al. 2014. WormBase 2014: new views of curated biology. Nucleic Acids Res 42: D789–93.

Hart AC. 2006. Behavior. WormBook. [Online] Available at: http://wormbook.org/chapters/www_behavior/behavior.html. Accessed on 5 May 2015.

Hemmerich PH, von Mikecz AH. 2013. Defining the subcellular interface of nanoparticles by live-cell imaging. PLoS One 8:e62018.

Honda Y, Tanaka M, Honda S. 2010. Trehalose extends longevity in the nematode *Caenorhabditis elegans*. Aging Cell 9:558–69.

Jung SK, Qu X, Aleman-Meza B, Wang T, Riepe C, Liu Z, et al. 2015. Multi-endpoint, high-throughput study of nanomaterial toxicity in *Caenorhabditis elegans*. Environ Sci Technol 49:2477–85.

Kaletta T, Hengartner MO. 2006. Finding function in novel targets: *C. elegans* as a model organism. Nat Rev Drug Discov 5:387–98.

Klein FA, Pastore A, Masino L, Zeder-Lutz G, Nierengarten H, Oulad-Abdelghani M, et al. 2007. Pathogenic and non-pathogenic polyglutamine tracts have similar structural properties: towards a length-dependent toxicity gradient. J Mol Biol 371:235–44.

Labbadia J, Morimoto RI. 2013. Huntington's disease: underlying molecular mechanisms and emerging concepts. Trends Biochem Sci 38:378–85.

Li H, Li SH, Yu ZX, Shelbourne P, Li XJ. 2001. Huntingtin aggregate-associated axonal degeneration is an early pathological event in Huntington's disease mice. J Neurosci 21:8473–81.

Linse S, Cabaleiro-Lago C, Xue WF, Lynch I, Lindman S, Thulin E, et al. 2007. Nucleation of protein fibrillation by nanoparticles. Proc Natl Acad Sci USA 104:8691–6.

Lints R, Hall DH.2009. Reproductive system, egglaying apparatus. WormAtlas [Online] Available at http://wormatlas.org/hermaphrodite/egglaying apparatus/Eggframeset.html. Accessed on 5 May 2015.

Lucchini RG, Dorman DC, Elder A, Veronesi B. 2012. Neurological impacts from inhalation of pollutants and the nose-brain connection. Neurotoxicology 33:838–41.

Mi H, Muruganujan A, Thomas PD. 2013. PANTHER in 2013: modeling the evolution of gene function, and other gene attributes, in the context of phylogenetic trees. Nucleic Acids Res 41:D377–86.

Morley JF, Brignull HR, Weyers JJ, Morimoto RI. 2002. The threshold for polyglutamine-expansion protein aggregation and cellular toxicity is dynamic and influenced by aging in *Caenorhabditis elegans*. Proc Natl Acad Sci USA 99:10417–22.

Nass R, Hall DH, Miller III DM, Blakely RD. 2002. Neurotoxin-induced degeneration of dopamine neurons in *Caenorhabditis elegans*. Proc Natl Acad Sci USA 99:3264–9.

Neudecker P, Robustelli P, Cavalli A, Walsh P, Lundström P, Zarrine-Afsar A, et al. 2012. Structure of an intermediate state in protein folding and aggregation. Science 336:362–6.

Pakhomov AA, Martynov VI. 2008. GFP family: structural insights into spectral tuning. Chem Biol 15:755–64.

Petrascheck M, Ye X, Buck LB. 2007. An antidepressant that extends lifespan in adult *Caenorhabditis elegans*. Nature 450:553–6.

Pluskota A, Horzowski E, Bossinger O, von Mikecz A. 2009. In *Caenorhabditis elegans* nanoparticle-bio-interactions become transparent: silica-nanoparticles induce reproductive senescence. PLoS One 4:e6622.

Ratnasekhar C, Sonane M, Satish A, Mudiam MK. 2015. Metabolomics reveals the perturbations in the metabolome of *Caenorhabditis elegans* exposed to titanium dioxide nanoparticles. Nanotoxicology. [Epub ahead of print].

Ross CA, Poirier MA. 2004. Protein aggregation and neurodegenerative disease. Nat Med 10:S10–17.

Schafer WF. 2006. Genetics of egg-laying in worms. Annu Rev Genet 40: 487–509.

Scharf A, Piechulek A, von Mikecz A. 2013. Effect of nanoparticles on the biochemical and behavioral aging phenotype of the nematode *Caenorhabditis elegans*. ACS Nano 7:10695–703.

Scherzinger E, Lurz R, Turmaine M, Mangiarini L, Hollenbach B, Hasenbank R, et al. 1997. Huntingtin-encoded polyglutamine expansions form amyloid-like protein aggregates *in vitro* and *in vivo*. Cell 90: 549–58.

Stiernagle T. 1999. Maintenance of *C. elegans*. In: Hope IA, ed. *C. elegans*. Oxford, New York: Oxford Biology Press, 51–67.

Tanaka M, Machida Y, Niu S, Ikeda T, Jana NR, Doi H, et al. 2004. Trehalose alleviates polyglutamine-mediated pathology in a mouse model of Huntington disease. Nat Med 10:148–54.

Tanis JE, Moresco JJ, Lindquist RA, Koelle MR. 2008. Regulation of serotonin biosynthesis by the G proteins Galphao and Galphaq controls serotonin signaling in *Caenorhabditis elegans*. Genetics 178: 157–69.

Tank EM, Rodgers KE, Kenyon C. 2011. Spontaneous age-related neurite branching in *Caenorhabditis elegans*. J Neurosci 31: 9279–88.

Trent C, Tsuing N, Horvitz HR. 1983. Egg-laying defective mutants of the nematode *Caenorhabditis elegans*. Genetics 104: 619–47.

Zhang M, Chung SH, Fang-Yen C, Craig C, Kerr RA, Suzuki H, et al. 2008. A self-regulating feed-forward circuit controlling *C. elegans* egg-laying behavior. Curr Biol 18:1445–55.

Supplementary material available online

Supplementary Figures S1 and S2, Videos S1–S3 and Tables S1–S3